Preparation and characterization of long-lived molecular Rydberg states: Application to HD

F. Merkt,[a] H. Xu, and R. N. Zare
Department of Chemistry, Stanford University, Stanford, California 94305

(Received 8 September 1995; accepted 11 October 1995)

The decay dynamics by predissociation and rotational autoionization of high Rydberg states of HD close to the first few rotational levels of the ground vibronic state of the HD^+ cation have been studied by delayed pulsed field ionization following resonant $(1+1')$ two-photon absorption via the B state. Although predissociation and autoionization both contribute to the rapid decay of Rydberg states with principal quantum number $n \ll 100$, the highest Rydberg states ($n > 100$) are stable for more than 20 μs. In contrast to H_2, channels associated with an HD^+ ($v^+=0$, $N^+=$even) ion core are coupled to channels associated with an HD^+ ($v^+=0$, $N^+=$odd) ion core. We demonstrate that complex resonances that arise from rotational channel interactions between low ($n \sim 25$) Rydberg states characterized by a core with rotational angular momentum quantum number $N^+ + 2$ and the pseudocontinuum of very high Rydberg states characterized by an N^+ core can be used with high efficiency to produce long-lived high Rydberg states. An investigation of the pulsed field ionization characteristics of these complex resonances enables us to measure the branching between diabatic and adiabatic field ionization and to determine the optimal conditions required to extend the method of H-photofragment Rydberg translational spectroscopy pioneered by Schnieder *et al.* [J. Chem. Phys. **92**, 7027 (1990)] to molecular species. © *1996 American Institute of Physics*. [S0021-9606(96)02103-1]

I. INTRODUCTION

The recent discovery of unexpectedly long-lived high Rydberg states in atoms and molecules constitutes an important development in physical chemistry.[1–13] The existence of these long-lived states has rendered possible the development and general applicability of new research tools for the study of molecules and ions in the gas phase such as zero kinetic energy photoelectron spectroscopy (ZEKE-PES),[14,15] mass-analyzed threshold ionization (MATI) spectroscopy,[16] and the preparation of state-selected ions.[17,18] The objective of this report is to demonstrate that high molecular Rydberg states are sufficiently long lived that the method of H-atom photofragment translational spectroscopy pioneered by Ashfold, Welge, and co-workers[19–25] can be generalized to probe the velocity distribution of other species in the gas phase than the hydrogen atom.

The success of this method resides in its ability to probe the H-atom product by exciting the product to a high Rydberg state instead of ionizing it, and subsequently to let the excited product travel, in a neutral Rydberg state, to the detector where it field ionizes. Because the H atom moves toward the detector as a neutral rather than an ion, its time of flight is not subject to distortions caused by Coulombic repulsions with other charged species created in the photodissociation volume or by stray fields. This advantage has enabled the study of dissociation processes that yield H atoms[19–23] and reactions that produce H atoms,[24,25] both with unprecedented resolution and sensitivity. Because it is restricted to the H atom, however, the method lacks the advantage of general applicability. The first step, reported here, toward a generalization of the technique to molecular products such as H_2 or HD consists of verifying that high Rydberg states of these molecules are sufficiently long lived. The next step, to be reported separately,[26] consists of taking advantage of these long lifetimes to measure the velocity distribution of a *molecular* reaction product. Our ultimate goal is to use this approach to measure the degree of alignment and orientation of the HD product in the state-resolved differential cross section of the reaction $H+D_2(v,J) \rightarrow HD(v',J')+D$.[27]

We report here on the spectroscopic and dynamical properties, including lifetimes and pulsed field ionization characteristics, of high Rydberg states of HD in an effort to determine which Rydberg states are long lived and under which experimental conditions. In addition to providing important new information on the *gerade*[28] Rydberg states of HD, which complements that of earlier investigations of the *ungerade* Rydberg states of HD[29,30] and of recent investigations of the *gerade* Rydberg states of H_2 by similar methods,[31,32] this study brings us to the conclusion that the long lifetimes of high Rydberg states of HD open the way to a new generation of experiments in gas-phase physical chemistry.

II. EXPERIMENT

The main characteristics of the apparatus have been described in detail previously.[33] Only details pertinent to this study are summarized here. The high Rydberg states of HD are populated by the resonant $(1+1')$ two-photon excitation sequence

[a]Permanent address: Laboratorium für Physikalische Chemie, ETH Zürich (Zentrum), CH-8092 Zürich, Switzerland.

 0021-9606/96/104(3)/950/12/$6.00

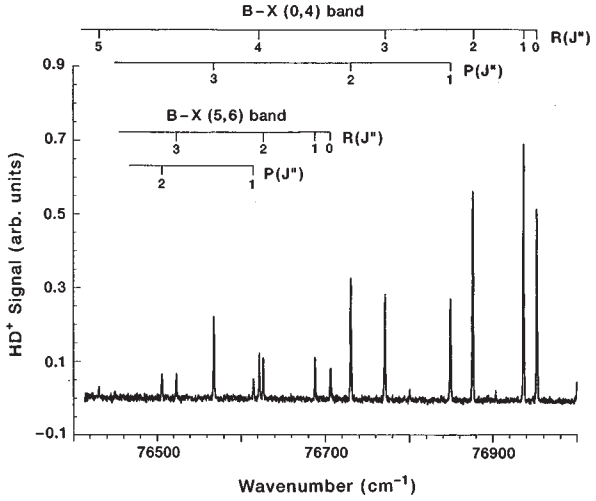

FIG. 1. $(1+1')$ REMPI spectrum of the $B-X$ transition between 76 400 and 77 000 cm^{-1}, revealing the (0,4) and (5,6) bands.

$$\mathrm{HD}\ X\ ^1\Sigma_g^+(v''=4,\ J'') \xrightarrow{\lambda_{\mathrm{VUV}}} \mathrm{HD}\ B\ ^1\Sigma_u^+(v'=0,\ J') \xrightarrow{\lambda_2} \mathrm{HD},\ \text{high}\ n. \quad (1)$$

Throughout this report, doubly primed quantities refer to the ground state in the excitation sequence (1), primed quantities to the intermediate state, and unprimed quantities to the high Rydberg states. The VUV radiation required to induce the first step in this sequence is generated by difference frequency mixing in a cell of krypton that is separated from the rest of the apparatus by a MgF_2 cylindrical lens. Because the laser beams cross it off center, this lens serves the joint purpose of separating the generated VUV radiation from the fundamental frequencies and of refocusing it into the ion-extraction region. The UV frequency required to drive the second step in the excitation sequence (1) is produced by frequency doubling the output of a Nd:YAG-pumped dye laser. The VUV and UV pulse energies are estimated to be 200 nJ and 12 mJ, respectively. The two copropagating lasers are linearly polarized, and the polarization vectors are arranged perpendicular to each other. Vibrationally excited HD $(v''=4, J'')$ is produced by flowing HD over the hot filament of an ion gauge 30 cm from the ionization region. The pressure in the ionization chamber is kept at 5×10^{-5} Torr when HD is flowing. Although the translational and rotational temperatures have thermalized to room temperature by the time the molecules have reached the ionization region, a significant degree of vibrational excitation persists, as evidenced from the observation of the (0,4) and (5,6) bands in the HD $B-X$ $(1+1')$ resonantly enhanced multiphoton ionization (REMPI) spectrum displayed in Fig. 1.

Predissociation in the high Rydberg states of HD excited by the multiphoton sequence (1) is induced by a coupling with the dissociative state of HD having the configuration $(1\sigma_u)^2$. This predissociation leads to the formation of a ground-state H $(n=1)$ or D $(n=1)$ atom and an excited H $(n=2)$ or D $(n=2)$ atom. This excited atom can easily be ionized in a single-photon process by the frequencies used in the excitation sequence (1). Information on the predissociation of HD occurring on the time scale of the photoexcitation (5 ns) can therefore be obtained by collecting the yield of ionized atomic fragments. Moreover, information on the competition between photodissociation and photoionization can be obtained by monitoring the yield of HD^+ and H^+ or D^+ ions produced. As a result, a complete picture of the decay of the high Rydberg states of HD can be reconstructed. This approach implies, however, that ions rather than electrons are monitored, because of the need to distinguish H^+ and HD^+ ions by their time of flight (TOF). The choice of detecting ions, however, imposes some restrictions on the information that can be obtained by delayed pulsed field ionization; indeed, in experiments that seek to distinguish ions produced by direct ionization from those produced by delayed pulsed field ionization of long-lived high Rydberg states, the application of a weak dc electric field is required. This field must be sufficiently small not to cause field ionization of the high Rydberg states being studied but large enough to separate spatially the high neutral Rydberg states from the promptly produced ions during the delay time that separates photoexcitation from pulsed field ionization (PFI). In addition, this weak electric field has some effect on the properties of the high Rydberg states under investigation.[2,10] These considerations require experimental care but, as shown below, do not cause serious limitations on the range of experiments described here.

Figures 2(a) and 2(b) illustrate the electric-field pulse sequences used to investigate the properties of the high Rydberg states of HD. Two pulsed electric fields are used; the first is optional. Depending on the timing of the experiment, photoexcitation can be carried out under field-free conditions [i.e., the first pulsed field is applied after the laser pulse, as in Fig. 2(a)] or in the presence of a weak dc field [i.e., the first pulsed field is applied before photoexcitation, as in Fig. 2(b)]. After a suitable delay time, a second, larger pulsed electric field is applied to field ionize the Rydberg states that have survived and to extract all generated ions along the TOF tube toward the detector. This sequence of electric fields is very versatile and renders possible the following three experiments, the outcomes of which are described in Sec. III.

(1) Photodissociation and photoionization study of HD in the vicinity of the ionization limit. In this experiment, photoexcitation is carried out under field-free conditions [Fig. 2(a)] to minimize blurring of the Rydberg structure by the Stark effect. Only one pulsed electric field (70 V/cm) is applied, typically 100 ns after photoexcitation. This electric field extracts all ions (HD^+, H^+, and D^+) produced by photoionization of HD or photoionization of the dissociation products $H(n=2)$ and $D(n=2)$, as explained above. Because of the different TOF of particles with mass 1, 2, and 3, photoionization and photodissociation spectra can be recorded separately.
(2) Determination of the pulsed field ionization characteris-

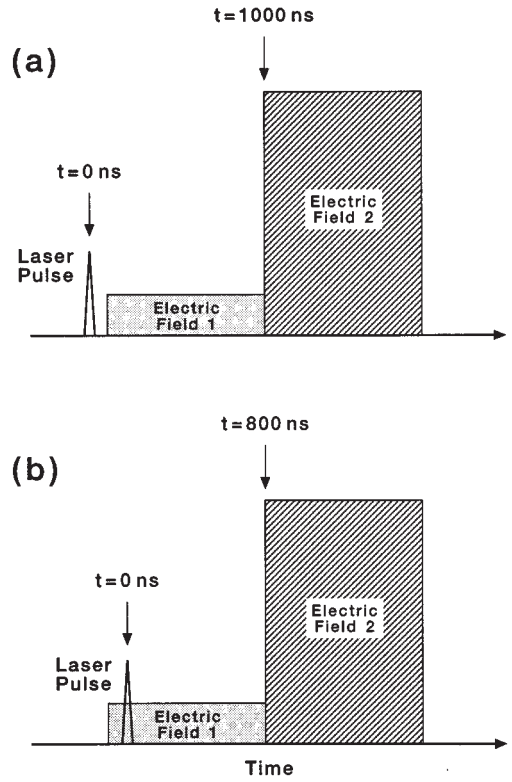

FIG. 2. Sequences of pulsed electric fields used to extract dynamical and spectroscopic information on the Rydberg states of HD. (a) Pulse sequence adapted for photoexcitation under field-free conditions. (b) Pulse sequence adapted for photoexcitation in the presence of a dc electric field.

tics of high Rydberg states of HD. Two electric fields are required for this measurement. The experiment is carried out by gradually increasing the magnitude of the first pulsed electric field (see Fig. 2) and monitoring the fraction of initially populated high Rydberg states that is not ionized by the first field and therefore survives until the application of the second, larger electric field. By applying the first pulsed field either before [as in Fig. 2(b)] or after [as in Fig. 2(a)] photoexcitation, we can study the ionization behavior by dc and pulsed electric fields.

(3) Lifetime measurement of high Rydberg states. This experiment also requires the use of two pulsed electric fields. The first field serves to displace spatially the ions produced by direct ionization or fast autoionization from the long-lived high Rydberg states. The decay of the initial population of these states is monitored by PFI as a function of the delay separating photoexcitation from the second pulsed field shown in Fig. 2.

III. RESULTS AND DISCUSSION

A. Photoionization and photodissociation of HD in the vicinity of the ionization threshold

Figures 3(a)–3(d) and 4(a)–4(d) show photoionization and photodissociation spectra of HD recorded via even and odd rotational states of the HD B state, respectively. The photodissociation spectra shown here are from the H^+ ion

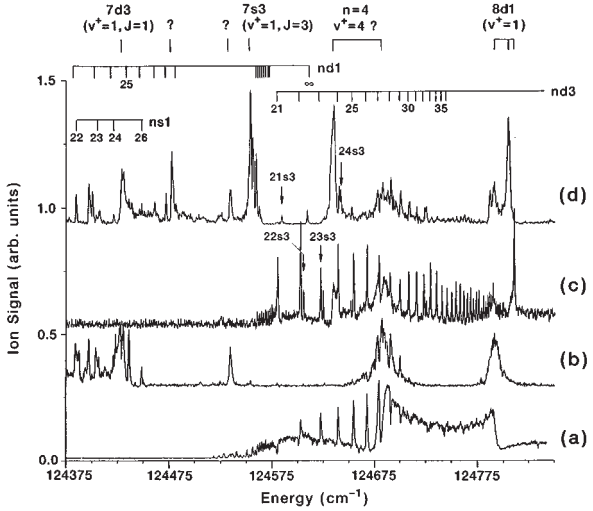

FIG. 3. Photoionization and photodissociation spectra of HD, detecting HD^+ and H^+, respectively, after two-photon excitation via the $B(v'=0, J'=0)$ intermediate state (panels a and b) and via the $B(v'=0, J'=2)$ intermediate state (panels c and d).

signal. The D^+ ion signal exhibits similar features and is therefore omitted. The reason for having separate displays of spectra recorded via even and odd rotational levels of the B state is that the parity selection rule dictates that absorption to s and d Rydberg states should be restricted to series that converge on even (odd) rotational levels of the ion when excitation occurs through an odd (even) rotational level of the B state. To make a direct comparison of the spectra recorded via different intermediate states, we referenced the energy scale on the horizontal axis to the ground neutral state $(v''=0, J''=0)$ of HD, using the available spectroscopic data on the X and B states of HD,[34,35] the well-characterized val-

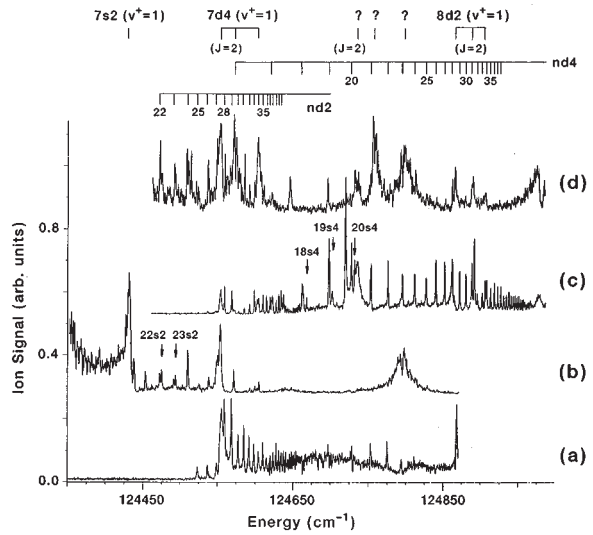

FIG. 4. Photoionization and photodissociation spectra of HD, detecting HD^+ and H^+, respectively, after two-photon excitation via the $B(v'=0, J'=1)$ intermediate state (panels a and b) and via the $B(v'=0, J'=3)$ intermediate state (panels c and d).

TABLE I. Rydberg series converging on the ground electronic state of HD^+ that are optically accessible via given intermediate rotational levels of the B state. The series are ordered according to which ionic rotational level they converge. The series indicated in brackets correspond to series not observable when the excitation is carried out from the $v''=4$, $J''=0$ ($M_{J''}=0$) ground state (see the text for details).

Ionization channel	$B(v'=0, J'=0)$	$B(v'=0, J'=1)$	$B(v'=0, J'=2)$	$B(v'=0, J'=3)$
$v^+=0, N^+=0$		$[ns0\ J=0]$ $nd0\ (J=2)$		$nd0\ (J+2)$
$v^+=0, N^+=1$	$ns1\ (J=1)$ $nd1\ (J=1)$		$ns1\ (J=1)$ $nd1\ (J=1)$ $nd1\ (J=2)$ $nd1\ (J=3)$	
$v^+=0, N^+=2$		$ns2\ (J=2)$ $[nd2\ (J=0)]$ $nd2\ (J=1)$ $nd2\ (J=2)$		$ns2\ (J=2)$ $nd2\ (J=2)$ $nd2\ (J=3)$ $nd2\ (J=4)$
$v^+=0, N^+=3$	$nd3\ (J=1)$		$ns3\ (J=3)$ $nd3\ (J=1)$ $nd3\ (J=2)$ $nd3\ (J=3)$	
$v^+=0, N^+=4$		$nd4\ (J=2)$		$ns4\ (J=4)$ $nd4\ (J=2)$ $nd4\ (J=3)$ $nd4\ (J=4)$
$v^+=0, N^+=5$			$nd5\ (J=3)$	
$v^+=0, N^+=6$				$nd6\ (J=4)$

ues for the ionization potential of HD,[36] and the calculated energy levels of the HD^+ ion,[37] when required.

Table I lists the Rydberg series converging on the ground electronic state of HD^+ that are optically accessible via given intermediate rotational levels of the B state. According to common practice, the series are labeled nlN^+, where n stands for the principal quantum number, l for the Rydberg electron orbital angular momentum quantum number, and N^+ for the rotational quantum number of the ionic state to which the series converge. In the presence of an electric field, the orbital angular momentum quantum number l is no longer well defined in sufficiently high Rydberg states. In this case, Rydberg states are labeled simply $n(N^+)$. The bracketed series in Table I indicate those that are not observable when the excitation is carried out from the $v''=4$, $J''=0$ ($M_{J''}=0$) ground state. In this case, the perpendicular polarization arrangement of our lasers leads to excitation to $M_J=1$ states, which is incompatible with the observation of $J=0$ final states. In the energy region close to the first ionization limit, the spectra are dominated by transitions to high Rydberg states converging on the lowest rotational levels of the ground vibronic state of the HD^+ cation with $N^+=0$–6. However, transitions to lower Rydberg states converging on higher vibrational states of HD^+ (referred to below as interlopers) are also expected, in particular the $n=7$ and 8 s/d Rydberg complexes of the series converging on $v^+=1$, the $n=4$ Rydberg complex of the series converging on $v^+=4$, and possibly the $n=3$ complex of the series converging on $v^+=8$. These interloper states generally lead to strong perturbations of the Rydberg series converging on the $v^+=0$ levels. Unlike in H_2, where an unambiguous identification of most interlopers appears possible with a simple l-uncoupling calculation,[32] such an identification could not be made in the present study, possibly because of the higher density of interlopers that results from the smaller rovibrational spacings in the HD^+ ion. Only tentative assignments of the interloper states are indicated in Figs. 3 and 4. In some cases, the total angular momentum quantum number J of the interlopers could be determined from a comparison of photodissociation/photoionization spectra recorded via different intermediate states. For instance, the $J=2$ character of the resonance observed at 124 735 cm^{-1} in Fig. 4(c) can be inferred from its presence in the photoionization spectrum recorded via $J=3$ but its absence from the spectra recorded via $J=1$ [Figs. 5(a) and 5(b)] and $J=5$ (not shown).

Several considerations need to be taken into account to correctly interpret the features observed in the spectra displayed in Figs. 3 and 4.

(1) The H^+ signal in Figs. 3(b), 3(d), 4(b), and 4(d) originates exclusively from one-photon ionization of excited atomic H ($n=2$) dissociation products with the laser frequencies used in the excitation sequence (1). This conclusion has two consequences. First, the experiment is insensitive to predissociation processes that yield two ground-state H (D) atoms. Second, the experiment reg-

isters only photodissociation processes that occur on a time scale of 5 ns, which corresponds to the temporal width of our laser pulses.

(2) The photoionization spectra represent the yield of HD^+ ions extracted by a pulsed electric field of 70 V/cm delayed approximately 100 ns with respect to photoexcitation. The HD^+ ions that contribute to the photoionization spectra can be formed by four distinct processes: direct ionization, autoionization, pulsed field ionization, and forced autoionization. The direct ionization yield is generally weak and contributes only a small, smooth background to the spectra. Most of the structure observed in the spectra above the $N^+=0$ threshold in Figs. 3(a) and 3(c) and 4(a) and 4(c) stems from rotational autoionization of Rydberg states that are coupled to the underlying continua; typical examples are the long $nd2$ and $nd3$ progressions observed in Figs. 4(a) and 4(c) and 3(a) and 3(c), respectively. Pulsed field ionization contributes to the HD^+ ion yield in the region below the $v^+=0$, $N^+=0$ ionization threshold, where Rydberg states are energetically unable to ionize in the absence of an electric field. Pulsed field ionization also occurs in narrow bands of $\sim 10\ cm^{-1}$ just below each successive ionization threshold, an observation that can be attributed to the long lifetimes ($\tau > 100$ ns) of high Rydberg states with $n>100$ belonging to series that converge on these thresholds. Assuming that the field ionization occurs adiabatically, the onset of the pulsed field ionization signal is expected to occur some $50\ cm^{-1}$ below the ionization threshold, i.e., for Rydberg states with principal quantum number $n>50$. In forced autoionization, Rydberg states with much lower n values than 50 ionize when the pulsed electric field is applied. Some examples are the $28d2$ and $22d3$ Rydberg states just below the $N^+=0$ and $N^+=1$ ionization limits, respectively. These states, which are coupled to the pseudocontinuum of high Rydberg states just below the $N^+=0$ ($N^+=1$) limit, autoionize only once the pseudocontinuum has been turned into an ionization continuum by the electric field. The electric field can help in this process by inducing or strengthening the coupling between the Rydberg state and the continuum that is just opening.[38] These resonances offer unique advantages because they have large oscillator strengths determined by their relatively low n character (the absorption cross section to Rydberg states scales as n^{-3}) and, at the same time, display the field ionization characteristics and the long lifetimes typical for the pseudocontinuum of high Rydberg states to which they are coupled (see Secs. III B and III C). Consequently, they provide an efficient means to produce large populations of stable neutral states that can be ionized easily by a small electric field. This property is precisely that required to extend the method of H-atom photofragment translational spectroscopy to probe molecular species. Because of the importance of this property, the nature of these resonances, referred to thereafter as complex resonances,[39] is characterized more extensively in Secs. III B and III C below.

The most complete and regular Rydberg series observed in the spectra displayed in Figs. 3 and 4 are the nd series converging on ionic rotational states with rotational quantum numbers $N^+=J'\pm 1$, where J' represents the total angular momentum of the rotational state selected in the B state. These series typically appear as long progressions of autoionizing resonances in the photoionization spectra. Examples are the $nd2$ series in Fig. 4(a) and the $nd2$ and $nd4$ series in Fig. 4(c) as well as the $nd1$ series in Fig. 3(a) and the $nd1$ and $nd3$ series in Fig. 3(c). The resolution of the lasers in the present study does not enable us to resolve nd Rydberg series of different total angular momentum J (see Table I).

The nd series converging on ionic rotational states with rotational quantum number $N^+=J'\pm 3$ are generally weak and of irregular intensity. When observed, these series appear to borrow their intensity from low n interlopers that belong to series converging on higher vibrational levels of HD^+; examples are the $nd4$ series in Fig. 4(a) and the $nd3$ series in Fig. 3(a).

The ns series converging on ionic rotational states with rotational quantum number $N^+=J'\pm 1$ and $N^+=J'\pm 3$ are present in most spectra, although they are much weaker than the nd, $N^+=J'\pm 1$ series and are of irregular intensity. No transition to an ns Rydberg state could be unambiguously identified beyond $n=35$.

The positions of the members of the s series are well described by the quantum defects (-0.1) derived for H_2 by Rottke and Welge.[31] The various components of the d series have quantum defects in the range between -0.03 and 0.05. The spectra represented in Figs. 3 and 4 contain no evidence of series with $l>2$.

Inspection of Figs. 3 and 4 reveals that the importance of predissociation diminishes above the ionization potential, where the photodissociation lines become less densely spaced, appear at irregular intervals, have irregular widths, and are broad in general. Moreover, the extended Rydberg series converging on rotational levels of the ground vibronic state of HD^+ appear almost exclusively in the photoionization spectra. These observations imply that the Rydberg series characterized by a $v^+=0$ ion core are not strongly predissociative but decay preferentially by (forced) autoionization or by pulsed field ionization when an electric field is applied. The scarce and irregular nature of the broad isolated resonances observed in the photodissociation spectra above the ionization threshold suggests strongly that these resonances stem from transitions to low-n interloper Rydberg states with vibrationally excited ion cores. The widths of these resonances lie in the range of 1–20 cm^{-1} and indicate that these interloper states are strongly coupled to the dissociation continua, an observation that can be attributed to the increasing overlap of the vibrational wave function of core states with $v^+>0$ with the repulsive potential of the $(1\sigma_u)^2$ configuration.

The strong predissociative nature of the low-n interlopers is often accompanied by a profound modification of the photoionization and photodissociation behavior of the series converging on the ground vibrational states of HD^+. The

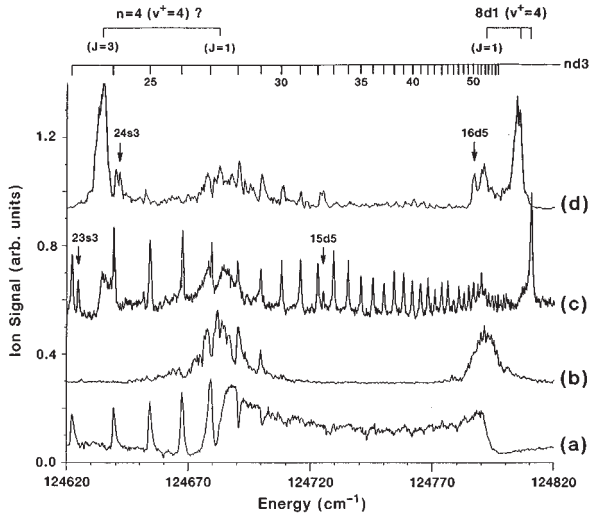

FIG. 5. Details of the photoionization and photodissociation spectra of HD, detecting HD^+ and H^+, respectively, after two-photon excitation via the $B(v'=0, J'=1)$ intermediate state (panels a and b) and via the $B(v'=0, J'=3)$ intermediate state (panels c and d).

presence of a neighboring dissociative interloper often causes these Rydberg states, which would normally appear only in the photoionization spectra, to decay by dissociation. When such a situation occurs, the interloper can safely be assumed to be coupled to the Rydberg series in question, an assumption that can assist, via perturbation rules, in the assignment of the interloper state.

A prominent example of an interaction between a low-n interloper state and high Rydberg states converging on the $v^+=0$ vibrational level is displayed in Figs. 5(a)–5(d), which show a detail of the photoionization and photodissociation spectra recorded via $B(J'=0$ and 2). At the position of the broad dissociation resonance centered at 124 682 cm^{-1} in Fig. 5(b), a complete change occurs in the photoionization spectrum [Fig. 5(a)]. The interloper resonance appears symmetric in the dissociation spectrum but is blue degraded in the photoionization spectrum. Members of the $nd3$ Rydberg series can be identified superimposed on the resonance. On the red side of the interloper, the $nd3$ Rydberg series (with $n=22$–25) appears as blue-degraded resonances in the photoionization spectrum. As the dissociative resonance is approached from below, the $nd3$ Rydberg series first becomes red degraded ($n=27$) and then goes over into window resonances ($n=28$–30). In the photodissociation spectrum, on the other hand, the $nd3$ resonances appear as dips below 124 682 cm^{-1} but as blue-degraded peaks on the high frequency side of the resonance. The next large resonance in the photodissociation spectrum, at 124 790 cm^{-1} in Figs. 3(b) and 5(b), displays a symmetric line shape in the dissociation spectrum but is red degraded in the photoionization spectrum. Because excitation is through the $B(v=0, J'=0)$ state, only final states with $J=1$ are optically accessible (see Table I) in the spectra represented in Figs. 3(a) and 3(b) and 5(a) and 5(b). When excitation occurs through $B(v=0, J'=2)$, final states with $J=2$–3 also become accessible. In this case, shown in Figs. 5(c) and 5(d), the $J=1$ structure described above is still recognizable, but the $J=2,3$ components of the $nd3$ Rydberg series appear with greater regularity both in the photodissociation and the photoionization spectra. Moreover, additional interloper states appear in dissociation at 124 804 cm^{-1} and in ionization at 124 810 cm^{-1}. A simple l-uncoupling calculation using case (b) quantum defects derived from the positions of the $n=3$ d Rydberg states of hydrogen listed in Ref. 35 suggests that the upper dissociative resonance in Fig. 5(b) be assigned to the $(v^+=1)$ $8d1$ $(J=1)$ Rydberg state.

The assignment of the lower dissociative resonance is less straightforward. Rydberg states converging on higher vibrational limits (e.g., $v^+=4$) as well as the $s-d$ series interaction might need to be taken into consideration to account for all the resonances found in this energy region. Modeling, by multichannel quantum defect theory (MQDT), the delicate balance between photoionization and photodissociation apparent in Figs. 3–5, as well as the complex changes in character observed in the various accessible channels, might provide a definitive assignment of the interloper states and lead to the determination of detailed couplings between open and closed channels. Conversely, the complex channel interactions apparent in these spectra may offer a useful testing ground for important developments in MQDT, which is presently able to treat autoionization and predissociation in a unified fashion.[40–42]

The overall features of the photodissociation and photoionization spectra of HD appear very similar to those obtained in the corresponding spectra of H_2 reported recently by Glab *et al.*[32] The same Rydberg series are observed, with similar quantum defects. Moreover, the H^+ (D^+) and H_2^+ (HD^+) ions are produced by similar mechanisms. Although the isotopic substitution first appears not to lead to significant modifications in the spectra other than those caused by the different rovibrational spacings in the two molecules, two important differences exist. The first is in the observation of D atomic fragments in addition to H atomic fragments in HD. In the energy range under investigation, however, no difference in the relative yield of excited H and D atoms could be detected within the limits of our resolution, sensitivity, and time scale. The second, more important, deviation concerns the onset of the HD^+ and H_2^+ ionization signals. When H_2 is excited through an even rotational level of the B state, the onset of the ionization signal occurs 80 cm^{-1} below the $v^+=0, N^+=1$ threshold (see Figs. 3 and 4 of Ref. 32) for the electric field used in Ref. 32. When, on the other hand, H_2 is excited through an odd rotational level of the B state, the onset of ionization is observed 80 cm^{-1} below the $v^+=0$, $N^+=0$ threshold (see Figs. 1 and 2 of Ref. 32). In HD, under our experimental conditions, the onset of the HD ion signal always takes place 50 cm^{-1} below the $v^+=0$, $N^+=0$ threshold (see Figs. 3 and 4), even when excitation occurs through even rotational levels of the B state. Such an observation can be explained only if the channels associated with an $HD^+(v^+=0, N^+=\text{odd})$ core are coupled to the channels associated with an $HD^+(v^+=0, N^+=\text{even})$ core. In other words, Rydberg states of HD converging on the $N^+=1$ and

three levels of HD^+ can rotationally autoionize to the $N^+=0$ and 2 continua, provided that these continua are energetically accessible. The autoionization process involves an odd change ΔN^+ in the core rotational angular momentum N^+. Such an autoionization process cannot be observed in H_2 or D_2 as a consequence of the forbidden nature of *ortho*-to-*para* interconversion processes. Further evidence for this autoionization process in HD involving an odd ΔN^+ change are presented in Sec. III C.

B. Pulsed field ionization characteristics of the $22d3 \leftrightarrow n \approx 106$ ($N^+=1$) complex resonance

To determine the pulsed field ionization characteristics of the $22d3 \leftrightarrow n \approx 106$ ($N^+=1$) complex resonance, we use two pulsed electric fields (Fig. 2), as outlined in Sec. II. The magnitude of the first field (duration 800 ns) is varied between 0 and 10 V/cm, whereas the magnitude of the second field is kept at 70 V/cm. At a fixed set of frequencies, corresponding to the excitation sequence

$$\mathrm{HD}\ \ X\ {}^1\Sigma_g^+(v''=4,\ J''=1) \xrightarrow{\lambda_{\mathrm{VUV}}} \mathrm{HD}\ \ B\ {}^1\Sigma_u^+(v'=0,\ J'=2) \xrightarrow{\lambda_2} \mathrm{HD},\qquad 22d3 \leftrightarrow n \approx 106 (N^+=1),$$

the TOF distribution of the HD^+ ions is monitored as the magnitude of the first electric field is gradually increased. The principle of the measurement relies on our ability to distinguish between the following two situations by analyzing the TOF profile of the HD^+ ions.

(1) The value of the first pulsed electric field is not high enough to field ionize the prepared Rydberg states that survive until they are ionized, and the generated ions extracted, by the second pulsed electric field in Fig. 2.
(2) The magnitude of the first pulsed electric field is sufficient to ionize the prepared Rydberg states. The ions produced by the first field are displaced toward the exit plate of the extraction region before the second pulsed electric field is applied. Their acceleration by the second field is therefore greatly reduced, and consequently their TOF to the detector becomes longer, compared with situation (1) above. The sequence of two electric fields shown in Figs. 1(a) and 1(b) offers, therefore, a means to determine the fraction of the initially prepared states that has not been ionized at a given value of the first electric field.

Two sets of experiments are carried out. In the first set, photoexcitation occurs under field-free conditions [see Fig. 2(a)]. The first pulsed field (800 ns duration) is applied typically 100 ns after photoexcitation and is immediately followed by the second pulsed field. In this case, the *pulsed electric field* ionization characteristics of the prepared Rydberg states are investigated. In the second set of experiments, photoexcitation occurs in the presence of the first electric field [see Fig. 2(b)]. Therefore, this set of experiments provides some information on the stability of high Rydberg states in dc *electric fields*.

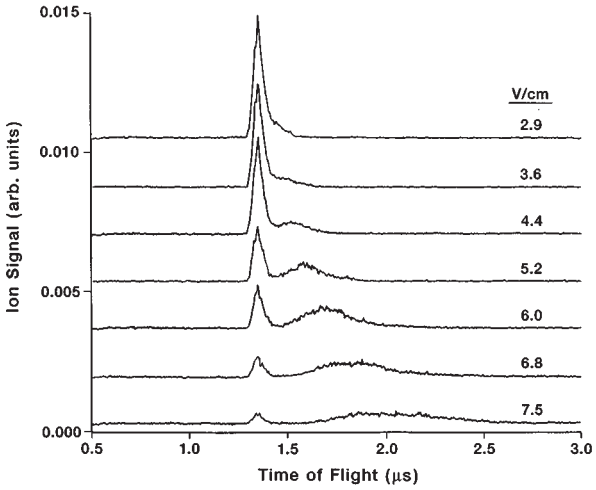

FIG. 6. Pulsed electric field ionization of the $n=22d3 \leftrightarrow n \approx 106 (N^+=1)$ complex resonance in HD. The HD^+ TOF profiles are obtained with the pulsed field sequence illustrated in Fig. 2(a). The early TOF peak corresponds to Rydberg states that are field ionized by the second pulsed field (70 V/cm), whereas the late TOF peak corresponds to Rydberg states that are ionized by the first pulsed field, the magnitude of which is indicated above the TOF profiles.

To illustrate the principle of the method, Fig. 6 shows TOF profiles obtained in the former series of experiments (photoexcitation carried out under field-free conditions) as the magnitude of the first electric field is increased from 2.9 to 7.5 V/cm. Similar profiles, not shown here, were obtained in the second set of experiments. All profiles consist of a sharp peak centered at 1.35 μs, which corresponds to Rydberg states that are field ionized by the second pulsed field [situation (1) above]. This peak is followed by a second, broader peak that corresponds to Rydberg states that have been field ionized by the first field [situation (2) above]. The maximum of this second peak is shifted to progressively longer TOF as the magnitude of the first pulsed field is increased. This behavior is expected because the ions produced by the first electric field are pushed further toward the exit plate of the extraction region, and therefore the ions are accelerated less by the second field, as the magnitude of the first field increases. The relative intensity of these two peaks provides a direct measure of the fraction of the initially populated states that have not been field ionized by the first field. This fraction is plotted as a function of the electric field strength in Fig. 7 (dotted line). The full line in Fig. 7 shows how this fraction varies when photoexcitation is carried out in the presence of a dc field. The difference between the two curves is striking: 90% ionization is achieved at an electric field strength of 8 V/cm when excitation occurs under field-free conditions, but it is achieved at a field strength of only 4 V/cm when the experiment is performed in the presence of a dc electric field.

Several observations are necessary to rationalize the field ionization behavior summarized in Fig. 7. Two distinct

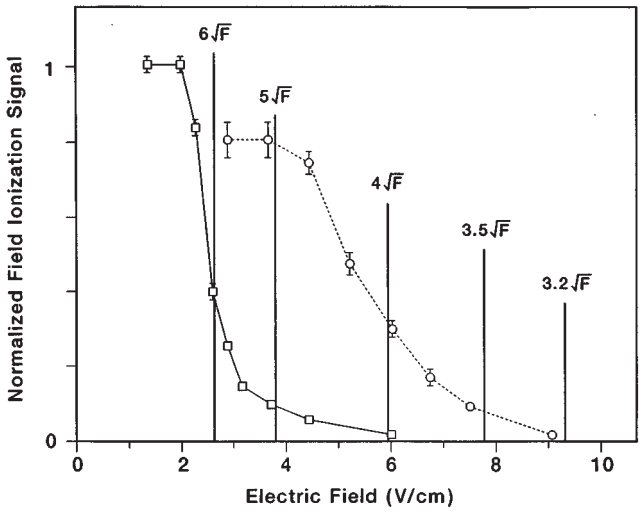

FIG. 7. Electric field ionization characteristics of the $n=22d3\leftrightarrow n\approx106(N^+=1)$ complex resonance in HD. The figure shows which fraction of the initial Rydberg population has not been field ionized as a function of the magnitude of the ionizing electric field. The dotted line describes ionization by a pulsed electric field, whereas the full line describes ionization by a continuous field. The vertical bars indicate the field at which ionization would be expected, for an $n=106$ Rydberg state, if it occurred at a sharp threshold given by $R/n^2=3.2\sqrt{F}$, $3.5\sqrt{F}$, $4\sqrt{F}$, $5\sqrt{F}$, and $6\sqrt{F}$, respectively.

mechanisms for the pulsed field ionization of Rydberg states can be observed[2,43,44] depending on the path followed by the Rydberg state on its way to ionization as the electric field increases. These mechanisms are known as adiabatic and diabatic field ionization. In adiabatic field ionization, the Stark state traverses adiabatically a long series of avoided crossings with other Stark states that belong to the same or other manifolds until the classical ionization limit is reached, at which point the Rydberg state ionizes. In this situation, ionization is expected to occur, for a Rydberg state of principal quantum number n, in a narrow range of electric fields F centered on the value given by

$$R/n^2=6.12\sqrt{F(\mathrm{V/cm})}, \tag{2}$$

where R is the Rydberg constant for HD in reciprocal centimeters. Equation (2) is also widely assumed to adequately describe the lowering of an ionization threshold by a dc electric field.

In diabatic field ionization, the Rydberg state traverses the curve crossings diabatically, and the Rydberg system ionizes at a field strength characteristic of its parabolic quantum numbers n, n_1, n_2, and m. A blueshifted ($n_1>n_2$) state ionizes at higher fields than a redshifted one ($n_2>n_1$). Moreover, states with increasing m values ionize at higher electric fields.[45] Diabatic field ionization of a Rydberg population prepared in a state of principal quantum number n under field-free conditions is expected to occur over a relatively wide range of electric field strengths given approximately by[2,43,44]

$$3.2\sqrt{F(\mathrm{V/cm})}<R/n^2<4.6\sqrt{F(\mathrm{V/cm})} \tag{3}$$

which reflects the different ionization thresholds of different Stark states. Field ionization of the hydrogen atom occurs diabatically. In other atomic systems, both adiabatic and diabatic ionization can be encountered; the former is more likely for states with low n and m quantum numbers and slowly rising electric fields, and the latter becomes increasingly important as n and m increase and at large electric field slew rates. Little is known about the field ionization behavior of molecular systems, although Rydberg states of molecules are generally assumed to behave as atomic Rydberg states and high Rydberg states with $n>100$ to ionize diabatically at electric-field slew rates in the range of 10^9–10^{11} V cm^{-1} s^{-1}.[2]

To facilitate interpretation of the field ionization characteristics of the $22d3\leftrightarrow n\approx106$ ($N^+=1$) complex resonance, the vertical bars in Fig. 7 have been placed to indicate the field at which ionization would be expected for an $n=106$ Rydberg state, if it occurred at a sharp threshold given by $R/n^2=3.2\sqrt{F}$, $3.5\sqrt{F}$, $4\sqrt{F}$, $5\sqrt{F}$, and $6\sqrt{F}$, respectively. The following conclusions can be derived from a close inspection of Fig. 7.

(1) The complex resonance composed of the interacting $22d3$ and $n\approx106$ ($N^+=1$) Rydberg states appears to display field ionization characteristics expected of an $n=106$ Rydberg state. Indeed, had the complex resonance retained a dominant $n=22$ character, no field ionization signal would have been observed, even with the second pulsed electric field.

(2) The *pulsed* field ionization (the dotted line in Fig. 7) appears to occur predominantly in the range predicted for diabatic field ionization [see Eq. (3) above], although 20% occur at lower electric fields, presumably adiabatically. Because the branching ratio of adiabatic/diabatic ionization decreases with increasing n, this observation suggests that more than 20% of the Rydberg states with $n<100$ ionize adiabatically under our experimental conditions (slew rate$\sim$2–5$\times10^8$ V cm^{-1} s^{-1}), which accounts for the observation made above that the onset of the pulsed field ionization signal in our spectra is consistent with the behavior predicted for adiabatic field ionization [see Eq. (2) above]. Xu, Helm, and Kachru[46] also observed adiabatic field ionization in Rydberg states of H_2 with $18<n<30$ at electric field slew rates of 1.33×10^{11} V cm^{-1} s^{-1}.

(3) A much higher dc electric field than given by Eq. (2) is required to ionize completely the excited Rydberg population (the solid line in Fig. 7) when photoexcitation is performed in the presence of a dc electric field. This observation indicates that stable Rydberg states ($\tau>1$ μs) exist above the classical field ionization limit given by Eq. (2). It also suggests that use of Eq. (2) to describe the lowering of an ionization threshold by a dc field must be made with caution. Indeed, Eq. (2) appears to describe adequately the low-frequency *onset* of an ionization signal, provided that part of the population ionizes adiabatically, but it fails to account for the shift of the blue edge of a peak in a pulsed field ionization spectrum recorded

in the presence of a dc field. This observation may be important for the technique of MATI spectroscopy, in which a dc electric field is commonly used to reject prompt ions.

C. Rydberg-state lifetime measurements

The observation made above (see Figs. 3 and 4), that Rydberg states converging on excited rotational levels of the HD^+ ion contribute to the photoionization spectrum even if they are located well below the field ionization range of the limit to which the series converges, indicates that relatively low Rydberg states, with principal quantum number in the range $20<n<100$, undergo rapid rotational autoionization and have lifetimes of less (probably much less) than 5 ns. Similarly, the predissociation spectra indicate that many Rydberg states with $n<100$ decay by predissociation on the nanosecond time scale or faster. The behavior of the high Rydberg states with $n>100$ stands in striking contrast to that of these lower Rydberg states. Indeed, the almost complete population of initially prepared states can be pulsed field ionized several microseconds after photoexcitation. This absence of continuity in the lifetimes between low and high Rydberg states has already been noted in several different systems including NO,[1,3,12] Ar,[7] and larger polyatomic molecules.[4–6,8,9,11] One interpretation is to invoke l and m_l mixing induced by external perturbations,[2,10,13] in particular, by stray inhomogeneous electric fields.[10] Another interpretation for molecular Rydberg states is to invoke interactions between the multipole moments of the core and the Rydberg electron.[47,48] These two interpretations need not be exclusive, although we suspect that the former often dominates in practical situations. The very high Rydberg states of HD probed in this study constitute another example of extreme stability.

Because of our interest in exploiting the long lifetimes of high Rydberg states to generalize the method of Rydberg TOF spectroscopy to the HD molecule, we desire to answer the following questions:

(1) What percentage of the initially prepared high Rydberg state population is long lived? If this percentage is small, serious limitations will be imposed on the sensitivity of this method.
(2) How long lived are high Rydberg states of HD, and what are the characteristics of their decay? Whether the lifetimes are 100 ns, 1, 10, or 100 μs will have some bearing on the design of experiments aimed at exploiting these lifetimes.

Additionally, we would like to be able to produce long-lived Rydberg states as efficiently as possible for experimental convenience. Therefore, we pay particular attention here to the behavior of complex resonances. As noted earlier, a complex resonance enables us to benefit simultaneously from the high oscillator strength to the low n interloper state and from some characteristics, including the pulsed field ionization behavior and the lifetimes, exhibited by the high Rydberg states to which this state is coupled. The sensitivity to the product to be probed by Rydberg TOF spectroscopy is therefore optimal at the positions of complex resonances.

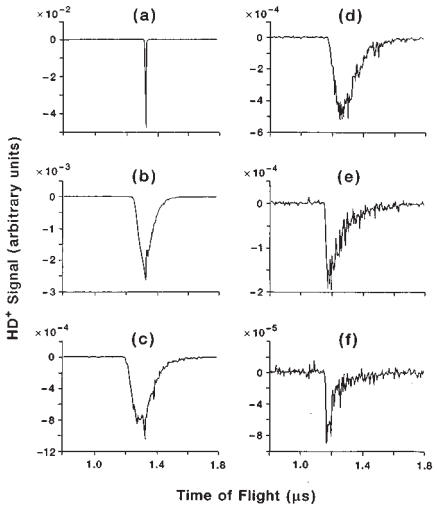

FIG. 8. Measurement of the decay of the $28d2 \leftrightarrow n \approx 110 (N^+=0)$ complex resonance by delayed pulsed field ionization. HD^+ TOF profiles obtained at delay times separating PFI from photoexcitation of (a) 100 ns, (b) 2.1 μs, (c) 4.1 μs, (d) 6.1 μs, (e) 12.1 μs, and (f) 20.1 μs. The horizontal TOF axis has been referenced to the time at which the second pulsed electric field is applied (see Fig. 2) and not to the time of photoexcitation so that all profiles can be compared directly. Note that the vertical scale has been adjusted to enhance features of the TOF profiles.

Although we have measured lifetimes of high Rydberg states converging on several limits and at different values of the principal quantum number n, we illustrate here in detail the measurement of the lifetime of the Rydberg state population produced following excitation to the $28d2 \leftrightarrow n \approx 110$ $(N^+=0)$ complex resonance. The decay of the initially prepared Rydberg states is monitored by measuring the magnitude of the pulsed field ionization signal as a function of the delay time between photoexcitation and the application of the pulsed electric field. A weak dc electric field (0.7 V/cm) is maintained in the extraction region to avoid the undesirable overlap of the HD^+ ion signal produced by pulsed field ionization with HD^+ ions formed before the electric field is applied. As demonstrated earlier, the latter ions have a longer TOF and can be distinguished from the former. In the $28d2 \leftrightarrow n \approx 110$ $(N^+=0)$ complex resonance, rotational autoionization is energetically impossible and no prompt ions are observed experimentally. Only predissociation needs to be considered as a source of decay of the initial population (fluorescence is assumed to take place on a slower timescale).

Figure 8 displays representative HD^+ TOF profiles obtained at different delay times separating PFI from photoexcitation. The horizontal TOF axis has been referenced to the time at which the second pulsed electric field is applied (see Fig. 2) and not to the time of photoexcitation so that all profiles can be compared directly. The vertical scale has been adjusted so as to reveal the TOF profiles with maximum detail. These profiles undergo two essential modifications as the delay time increases from 100 ns to 20 μs. First, the magnitude of the signal decreases monotonically, reaching

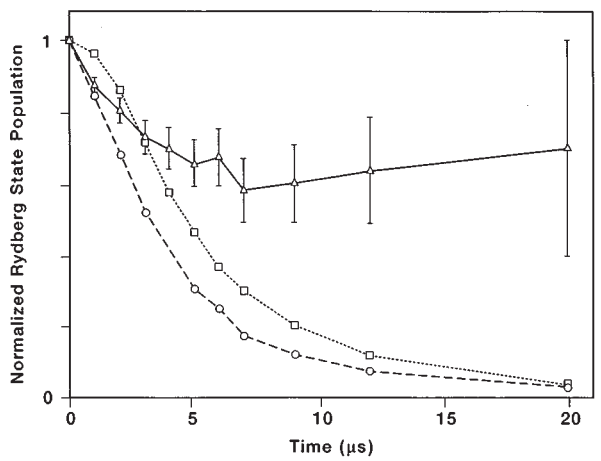

FIG. 9. Determination of the decay of the $28d2 \leftrightarrow n \approx 110(N^+=0)$ complex resonance. The curve reflecting the actual decay (full line) is obtained by dividing the integrated raw experimental signal intensities (dashed line) by the fraction of the population that can reach the detector assuming infinite lifetime, derived from the Monte Carlo simulation (dotted line).

2% of the initial value at 20 μs. Second, the shape of the peaks undergoes a rapid change, becoming broader at first, then asymmetric, and finally sharp again. Some care is required to extract a decay from these profiles. Indeed, the decay of the Rydberg states is not the only cause of the gradual loss of signal observed in Fig. 8. An important source of signal loss originates from the decreasing transmission function of the TOF spectrometer with increasing delay time. The HD molecules probed have a translational temperature of 298 K, and their velocity distribution is such that only a fraction can reach the detector at longer delay times. This unwanted contribution to the apparent decay must be deconvoluted to derive actual lifetimes.[49] Such a deconvolution was achieved by means of a Monte Carlo simulation of the TOF profiles.

The simulation, which took the geometry of the extraction and TOF tubes into account, was refined until all features of all profiles obtained in Fig. 8 could be simulated quantitatively. The quantitative agreement obtained between calculated and experimental profiles enabled us to evaluate the transmission function of the spectrometer accurately and to reconstruct the actual decay of the Rydberg state population. The procedure, illustrated in Fig. 9, consists of evaluating, by simulation, the fraction of the total population that can reach the detector assuming infinite lifetime for the Rydberg states (the dotted line in Fig. 9), and then dividing the integrated raw experimental signal intensities (the dashed line in Fig. 9) by this fraction to obtain the curve reflecting the actual decay (the full line in Fig. 9). The growing error bars with increasing delay time, which stem primarily from the decreasing signal strength, rule out a quantitative determination of the decay beyond 10 μs. Approximately 35% of the population decays within 8 μs, after which time no decay is observed within the limits of our sensitivity and time scale. The lifetime ($1/e$ time) is therefore too long to be measured in our setup and meets the condition $\tau > 20$ μs. We attribute the decay measured experimentally to slow predissociation of the complex resonance, and its multiexponential nature to a varying degree of state mixing in the Rydberg population, in good accord with the theoretical predictions of Ref. 10. The importance of predissociation in the decay measured experimentally is further indicated by the observation of weak H^+ and D^+ peaks in the TOF spectra measured at the shortest delay times.

Because ions, and not electrons, are monitored in these experiments, we are confident that we measure the decay of the *total* population that was optically prepared and not just a fraction of it. We can therefore rule out the importance, in this system, of the significant submicrosecond component in the decay predicted theoretically in Ref. 47. Moreover, the lifetime measured experimentally is amply sufficient to apply the method of Rydberg TOF spectroscopy to this system.

The lifetime measurement of Rydberg states can, in some cases, provide information on the decay mechanism. To illustrate this point, we summarize in Table II the results of a series of lifetime measurements at six different energetic positions near the $v^+=0$, $N^+=1$ ionization threshold. In all cases, excitation is carried out via the $B(v'=0, J'=2)$ intermediate state, and the photoionization and photodissociation spectra [Figs. 3(c) and 3(d)] are dominated by s and d Rydberg series converging on the $N^+=1$ and $N^+=3$ ionization thresholds. Table II also lists Rydberg states accessed at these energies, the energy relative to the $N^+=0$ and $N^+=1$ thresholds, and the measured stability of the Rydberg population. Figures 10(a)–10(d) show representative HD^+ TOF spectra,

TABLE II. Experimental determination of Rydberg state stabilities at various energetic positions, listed in the first column, near the $v^+=0$, $N^+=1$ ionization threshold. The Rydberg states that are accessed at these energies are listed in the second column. The third and fourth columns indicate the energy relative to the $N^+=0$ and $N^+=1$, respectively. The last column contains the measured lifetime of the Rydberg population.

Energy/cm^{-1}	Rydberg state	$\Delta E(N^+=0)$/cm^{-1}	$\Delta E(N^+=1)$/cm^{-1}	($1/e$) time/μs
124 560.3	$n=46$ ($N^+=1$)	−8.2	−52.0	>10
124 564.5	$n=48$ ($N^+=1$)	−4.0	−47.8	<1
124 602.7	$22d3$	Continuum	−9.6	>10
	$n=106$ ($N^+=1$)			
124 605.5	$22s3$	Continuum	−6.8	>10
	$n=126$ ($N^+=1$)			
124 606.3	$n=134$	Continuum	−6.0	>10
124 617.3	⋯	Continuum	Continuum	⋯

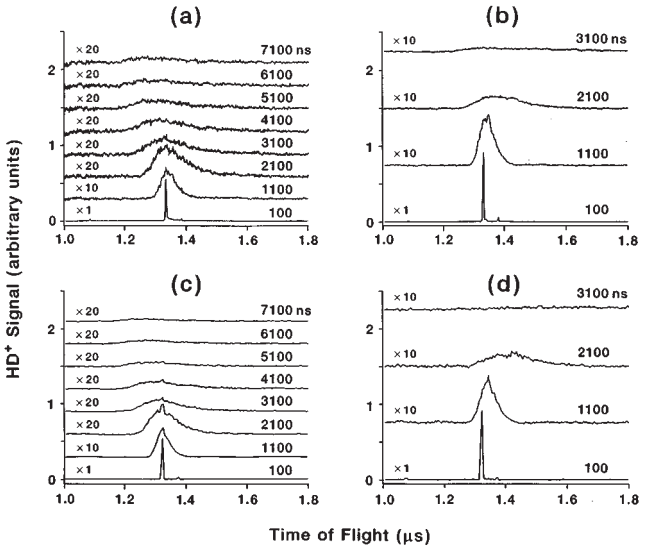

FIG. 10. Measurement of Rydberg state decay in the vicinity of the $v^+=0$, $N^+=1$ ionization threshold. HD^+ TOF spectra are shown (panel a), obtained at successive delay times, corresponding to excitation to the $n=46$ ($N^+=1$) Rydberg states, (panel b) the $n=48$ ($N^+=1$) Rydberg states, the $n=22d3\leftrightarrow n\approx 106(N^+=1)$ complex resonance (panel c), and the continuum above the $N^+=1$ threshold (panel d).

obtained at successive delay times, that correspond to excitation to the $n=46$ ($N^+=1$) Rydberg states, the $n=48$ ($N^+=1$) Rydberg states, the $n=22d3\leftrightarrow n\approx 106(N^+=1)$ complex resonance, and the continuum above the $N^+=1$ threshold, respectively. When excitation occurs directly to the continuum [Fig. 10(d)], the peak in the TOF profile moves toward longer times as the delay time (indicated above each TOF profile) increases, as expected for prompt ions (see Sec. III B). At 4 μs delay, all ions have been swept out of the extraction region and no signal can be detected. At the position of the $n=22d3\leftrightarrow n\approx 106(N^+=1)$ complex resonance [Fig. 10(c)] and of the $n=46$ ($N^+=1$) Rydberg states [Fig. 10(a)], on the other hand, the HD^+ peak follows the pattern typical of long-lived Rydberg states described above (see Fig. 8); no prompt ions are produced and the decay is extremely slow.

Surprisingly, at the position of the $n=48$ ($N^+=1$) Rydberg state [Fig. 10(b)], the TOF profiles are identical to those obtained in the continuum above the $N^+=1$ threshold and radically different from those obtained at the position of the $n=46$ ($N^+=1$) Rydberg state. From the measurement in Fig. 10(b), we can conclude that these states decay by ionization in less than 1 μs. As can be seen in Table II, the position of the $n=48$ Rydberg state lies 49 cm^{-1} below the field-free $N^+=1$ ionization threshold but only 4.8 cm^{-1} below the $N^+=0$ ionization threshold. Ionization of this state is therefore energetically impossible in the absence of an electric field. The 0.7 V/cm field used in the experiment is strong enough to make the $N^+=0$ continuum accessible at the position of the $n=48$ ($N^+=1$) state but much too weak to make the $N^+=1$ continuum accessible. We must therefore conclude that this Rydberg state rotationally autoionizes to the $N^+=0$ continuum in a process involving an odd ΔN^+ change in core rotational angular momentum, an observation that supports the conclusion drawn at the end of Sec. III A from the onset of the ionization signal. Given that it is forbidden in H_2, the occurrence of this autoionization coupling in HD can only be attributed to the distinguishability of the two nuclei, as well as the breakdown of the parity and g/u symmetries induced in high Rydberg states by electric fields.

IV. CONCLUSIONS

Spectroscopic and dynamical properties of *gerade* Rydberg states of HD located close to the first ionization limit have been investigated following resonant two-photon absorption via selected rotational levels of the *B* state. The two frequencies used to excite the HD molecule to high Rydberg states also serve the purpose of ionizing the excited H ($n=2$) and D($n=2$) atoms that result from the predissociation of the Rydberg states. Photodissociation and photoionization spectra of HD are recorded separately by measuring the relative yield of H^+ and HD^+ ions as a function of the excitation frequencies. The overall features of the decay of the *gerade* Rydberg states of HD can be extracted from the analysis of these spectra. Finer details are obtained by measuring the lifetimes and the pulsed field ionization characteristics of Rydberg states located at several positions above and below the first ionization limits.

The main conclusions of this study can be summarized as follows:

(1) High Rydberg states of HD belonging to series converging on the ground vibronic state of HD are not strongly predissociative but decay preferentially by autoionization. Predissociation signals are commonly observed below the lowest ionization limit ($v^+=0$, $N^+=0$). Above the lowest ionization limit, predissociation is observed only when these series are perturbed by lower interloper Rydberg states that belong to series converging on excited vibrational levels of the ion. At the position of these interloper states, the competition between autoionization and predissociation gives rise to very complex spectral features (See Fig. 5).

(2) The behavior of the *gerade* Rydberg states of HD follows closely that observed in H_2 by Glab *et al.*,[32] with one exception: rotational autoionization processes involving an odd change in core rotational angular momentum are observed in HD but not in H_2, as a consequence of the forbidden nature of *ortho*-to-*para* interconversion processes in the latter molecule.

(3) The complex resonance composed of the interacting $22d3$ and $n\approx 106$ ($N^+=1$) Rydberg states displays the field ionization characteristics expected of an $n=106$ Rydberg state. The *pulsed* field ionization occurs predominantly in the electric field range predicted for diabatic field ionization although 20% occur at lower electric fields, presumably adiabatically. Because the branching ratio of adiabatic/diabatic ionization decreases with increasing n, we conclude that more than 20% of the Rydberg states of HD with $n<100$ ionize adiabatically under our experimental conditions (slew rate~ 2–5×10^8

V cm^{-1} s^{-1}). We also observe the existence of stable Rydberg states ($\tau > 1$ μs) above the classical field ionization limit. Although the classical model for field ionization describes adequately the low-frequency *onset* of a pulsed field ionization signal, provided that part of the population ionizes adiabatically, it fails to account for the shift of the blue edge of a peak in a delayed pulsed field ionization spectrum recorded in the presence of a dc field. This observation of stable Rydberg states above the classical field ionization limit may be important for the technique of mass-analyzed threshold ionization (MATI) spectroscopy in which a dc electric field is commonly used to reject prompt ions.

(4) In sharp contrast to Rydberg states with principal quantum numbers $n \ll 100$, which decay very rapidly either by autoionization or predissociation, Rydberg states located just below each ionization threshold ($n > 100$) have lifetimes that are too long to be measured with our apparatus ($\tau > 10$ μs).

(5) The very long lifetimes observed for the highest Rydberg states imply that the method of H-atom Rydberg photofragment translational spectroscopy can be generalized to probe molecular species. Complex resonances that result from the interaction between the pseudocontinuum of high Rydberg states located just below an ionic rotational level and relatively low Rydberg states ($n < 30$) belonging to series converging on higher-lying ionic rotational levels appear particularly attractive to achieve this goal. Indeed, at the position of these complex resonances, simultaneous benefit results from the large oscillator strength to the low-n interloper state (implying optimal sensitivity to the HD molecule) and from the long lifetimes and the field ionization characteristics of the high Rydberg states to which this interloper state is coupled.

ACKNOWLEDGMENTS

We express our deep gratitude to Neil E. Shafer-Ray for technical help in carrying out these measurements. F.M. gratefully acknowledges the financial support of the Fonds National Suisse de la Recherche Scientifique. This work was supported by the US National Science Foundation under Grant No. NSF CHE 93-22690.

[1] G. Reiser, W. Habenicht, K. Müller-Dethlefs, and E. W. Schlag, Chem. Phys. Lett. **152**, 119 (1988).
[2] W. A. Chupka, J. Chem. Phys. **98**, 4520 (1993).
[3] S. T. Pratt, J. Chem. Phys. **98**, 9241 (1993).
[4] X. Zhang, J. M. Smith, and J. L. Knee, J. Chem. Phys. **99**, 3133 (1993).
[5] H. Krause and H. J. Neusser, J. Chem. Phys. **99**, 6278 (1993).
[6] D. Bahatt, U. Even, and R. D. Levine, J. Chem. Phys. **98**, 1744 (1993).
[7] F. Merkt, J. Chem. Phys. **100**, 2623 (1994).
[8] W. G. Scherzer, H. L. Selzle, E. W. Schlag, and R. D. Levine, Phys. Rev. Lett. **72**, 1435 (1994).
[9] U. Even, R. D. Levine, and R. Bersohn, J. Phys. Chem. **98**, 3472 (1994).
[10] F. Merkt and R. N. Zare, J. Chem. Phys. **101**, 3495 (1994).
[11] H. J. Dietrich, R. Lindner, and K. Müller-Dethlefs, J. Chem. Phys. **101**, 3399 (1994).
[12] M. J. J. Vrakking and Y. T. Lee, Phys. Rev. A **51**, R894 (1995).
[13] J. Jortner and M. Bixon, J. Chem. Phys. **102**, 5637 (1995).
[14] K. Müller-Dethlefs and E. W. Schlag, Annu. Rev. Phys. Chem. **42**, 109 (1991).
[15] F. Merkt and T. P. Softley, Int. Rev. Phys. Chem. **12**, 205 (1993).
[16] L. Zhu and P. Johnson, J. Chem. Phys. **94**, 5769 (1991).
[17] F. Merkt, S. R. Mackenzie, and T. P. Softley, J. Chem. Phys. **99**, 4213 (1993).
[18] S. R. Mackenzie and T. P. Softley, J. Chem. Phys. **101**, 10609 (1994).
[19] L. Schnieder, W. Meier, K. H. Welge, M. N. R. Ashfold, and C. M. Western, J. Chem. Phys. **92**, 7027 (1990).
[20] G. P. Morley, I. R. Lambert, M. N. R. Ashfold, K. N. Rosser, and C. M. Western, J. Chem. Phys. **97**, 3157 (1992).
[21] M. N. R. Ashfold, I. R. Lambert, D. H. Mordaunt, G. P. Morley, and C. M. Western, J. Phys. Chem. **96**, 2938 (1992).
[22] D. H. Mordaunt, I. R. Lambert, G. P. Morley, M. N. R. Ashfold, R. N. Dixon, C. M. Western, L. Schnieder, and K. H. Welge, J. Chem. Phys. **98**, 2054 (1993).
[23] S. H. S. Wilson, J. D. Howe, K. N. Rosser, M. N. R. Ashfold, and R. N. Dixon, Chem. Phys. Lett. **227**, 456 (1994).
[24] L. Schnieder, K. Seekamp-Rahn, F. Liederer, H. Steuwe, and K. H. Welge, Faraday Discuss. Chem. Soc. **91**, 259 (1991).
[25] L. Schnieder, K. Seekamp-Rahn, J. Borkowski, E. Wrede, K. H. Welge, F. J. Aoiz, L. Banares, M. J. D'Mello, V. J. Herrero, V. Saez Rabanos, and R. E. Wyatt, Science **296**, 207 (1995).
[26] H. Xu, N. E. Shafer-Ray, F. Merkt, D. J. Hughes, M. Springer, R. P. Tuckett, and R. N. Zare, J. Chem. Phys. **103**, 5157 (1995).
[27] N. E. Shafer-Ray, A. J. Orr-Ewing, and R. N. Zare, J. Phys. Chem. **99**, 7891 (1995).
[28] The *gerade/ungerade* symmetry is only approximate in HD. Nevertheless, the g/u notation is useful and enables the same electronic states to have identical symmetry labels in HD and H_2.
[29] P. M. Dehmer and W. A. Chupka, J. Chem. Phys. **79**, 1569 (1983).
[30] N. Y. Du and C. H. Greene, J. Chem. Phys. **85**, 5430 (1986).
[31] H. Rottke and K. H. Welge, J. Chem. Phys. **97**, 908 (1992).
[32] W. L. Glab, K. Qin, and M. Bistransin, J. Chem. Phys. **102**, 2338 (1995).
[33] N. E. Shafer, H. Xu, R. P. Tuckett, M. Springer, and R. N. Zare, J. Phys. Chem. **98**, 3369 (1994).
[34] I. Dabrowski and G. Herzberg, Can. J. Phys. **54**, 525 (1976).
[35] K. P. Huber and G. Herzberg, *Molecular Spectra and Molecular Structure IV: Constants of Diatomic Molecules* (Van Nostrand, New York, 1979).
[36] J. M. Gilligan and E. E. Eyler, Phys. Rev. A **46**, 3676 (1992).
[37] R. E. Moss, Mol. Phys. **78**, 371 (1993).
[38] F. Merkt, H. H. Fielding, and T. P. Softley, Chem. Phys. Lett. **202**, 153 (1993).
[39] Ch. Jungen and M. Raoult, Faraday Discuss. Chem. Soc. **71**, 253 (1981).
[40] S. Ross and Ch. Jungen, Phys. Rev. Lett. **59**, 1297 (1987).
[41] S. Ross and Ch. Jungen, Phys. Rev. A **49**, 4353 (1994).
[42] S. Ross and Ch. Jungen, Phys. Rev. A **49**, 4364 (1994).
[43] *Rydberg States of Atoms and Molecules*, edited by R. F. Stebbing and F. B. Dunning (Cambridge University Press, New York, 1983).
[44] T. F. Gallagher, *Rydberg Atoms* (Cambridge University Press, Cambridge, 1994).
[45] W. E. Cooke and T. F. Gallagher, Phys. Rev. A **17**, 1226 (1978).
[46] E. Y. Xu, H. Helm, and R. Kachru, Phys. Rev. Lett. **59**, 1096 (1987).
[47] E. Rabani, R. D. Levine, A. Mühlpfordt, and U. Even, J. Chem. Phys. **102**, 1619 (1995).
[48] E. Rabani and R. D. Levine (unpublished).
[49] N. E. Shafer-Ray, H. Xu, M. Springer, and R. N. Zare (unpublished).